Adsorption Characterization of Lead(II) and Cadmium(II) on Crosslinked Carboxymethyl Starch

Yan Xiao Chen, Ben He Zhong, Wei Mao Fang

Chemical Engineering Institute, Sichuan University, Chengdu 610065, China

ABSTRACT: The adsorption of Pb(II) and Cd(II) ions with crosslinked carboxymethyl starch (CCS) was investigated as function of the solution pH, contact time, initial metal-ion concentration, and temperature. Isotherm studies revealed that the adsorption of metal ions onto CCS better followed the Langmuir isotherm and the Dubinin–Radushkevich isotherm with adsorption maximum capacities of about 80.0 and 47.0 mg/g for Pb(II) and Cd(II) ions, respectively. The mean free energies of adsorption were found to be between 8 and 16 kJ/mol for Pb(II) and Cd(II) ions; this suggested that the adsorption of Pb(II) and Cd(II) ions onto CCS occurred with an ion-exchange process. For two-target heavy-metal ion adsorption, a pseudo-second-order model and intraparticle diffusion seem significant in the rate-controlling step, but the pseudo-second-order chemical reaction kinetics provide the best correlation for the experimental data. The enthalpy change for the process was found to be exothermic, and the ΔS^{θ} values were calculated to be negative for the adsorption of Pb(II) and Cd(II) ions onto CCS. Negative free enthalpy change values indicated that the adsorption process was feasible. The studies of the kinetics, isotherm, and thermodynamics indicated that the adsorption of CCS was more effective for Pb(II) ions than for Cd(II) ions. © 2011 Wiley Periodicals, Inc. J Appl Polym Sci 124: 5010–5020, 2012

Key words: adsorption; crosslinking; kinetics (polym.); thermodynamics

INTRODUCTION

Water pollution due to toxic metals and organic compounds remains a serious environmental and public problem. Moreover, faced with more and more stringent regulations, water pollution has also become a major source of concern and a priority for most industrial sectors. Heavy-metal ions are often found in the environment as a result of their wide industrial use. They are common contaminants in wastewater, and many of them are known to be toxic or carcinogenic. For example, lead and cadmium are known as two of the most toxic metals and are very damaging to the environment. In addition, heavy metals are not biodegradable and tend to accumulate in living organisms, causing various diseases and disorders. Therefore, their presence in the environment, in particular, in water, should be controlled.

Adsorption is now recognized as an effective, efficient, and economic method for water-decontamination applications and for separation analytical purposes. The adsorbents may be of mineral, organic, or biological origin; activated carbons,[1,2] clay minerals,[3] agricultural wastes,[4] industrial byproducts,[5] biomass,[6,7] and polymeric materials[8,9] are significant examples. Despite their effectiveness as adsorbents, potential problems associated with their use is the lack of biodegradability and high operation cost. In this respect, the development of substitutes based on natural polysaccharides and their derivatives containing the required functional groups can be more attractive from a biodegradability point of view, and an important factor here will be matching the performance.

Of all of these natural polysaccharides, starch appears to be a very fascinating material for adsorption research, with high possibilities for wastewater treatment, and this application would enlarge the range of its utilization. It is well known that starch, which is an abundant, renewable, and biodegradable resource, has the capacity to associate by physical and chemical interactions with a wide variety of molecules. Hence, adsorption on starch derivatives can be a low-cost procedure of choice in water decontamination for the separation of compounds and a useful tool for protecting the environment.

Modified starch as an adsorbent has been intensively studied and has received much attention over past decades in wastewater treatment. Zhang and Chen[10] reported that crosslinked starch graft copolymers containing amine groups were efficient as adsorbents for Pb(II) and Cu(II) ions. Dong et al.[11] investigated crosslinked amino starch as an adsorbent

for Cr(VI) and Cu(II). Guo et al.[12] investigated the adsorption behavior of crosslinked starch phosphates for Zn(II) and found that the adsorption process followed the Langmuir isotherm and was endothermic in nature. Ding et al.[13] prepared dialdehyde 8-amino-quinoline starch and used it as a chelating agent for the removal of Zn(II) ions. Xie et al.[14] synthesized amino-modified starch via a grafting polymerization and ring-opening reaction using cassava starch as a raw material and used it as an adsorbent for the removal of Cd(II) ions from aqueous solution.

Although the past works have indicated that modified starch could be an effective adsorbent for wastewater treatment, there has been very little work undertaken examining the adsorption kinetics of crosslinked carboxymethyl starch (CCS) for Pb and Cd ions in detail. The underlying aim of this work was to emphasize the sorption kinetics of Pb and Cd ions on CCS and to show the importance of investigating the kinetics of adsorption to fully understand the adsorption phenomena. On the basis of the results related to adsorption behavior, the adsorption isotherm was interpreted with the help of the Langmuir, Freundlich, and Dubinin–Radushkevick (D–R) models to best fit the adsorption behavior. Thermodynamic parameters, such as the enthalpy of adsorption, entropy change of adsorption (ΔS^{θ}), and free energy change (ΔG^{θ}), were calculated and interpreted.

EXPERIMENTAL

Materials

Corn starch (industrial grade) was purchased from Dacheng Corn Starch Co., Ltd. (Jilin, China). Metal salts of $Pb(NO_3)_2$ and $CdCl_2 \cdot H_2O$ (Kelong Chemicals Co., Chengdu, China) were used to prepare metal-ion solutions. The solutions (1000 mg/L) were prepared by the dissolution of appropriate amounts of metal salts in doubly distilled water. The working solutions were prepared by the dilution of the stock solutions to appropriate volumes. Epichlorohydrin, sodium monochloroacetate, sodium hydroxide, and the other chemicals used in this study were analytical grade.

Preparation of CCS

CCS was prepared according to the method described in a previous work.[15] The degree of cross-linking of crosslinked starch was 440AGU/CL (crosslinking bond), where AGU is α-glucose. The degree of substitution of carboxymethyl groups was calculated as described in the a previous book.[16]

The sample with the degree of substitution of carboxymethyl groups of 0.10 was prepared to be used as the adsorbent. The sample was named CCS. The parameters of the pore structure of CCS, such as

TABLE I
ICP–AES Operating Conditions and Measurement Parameters

Parameter	
Radio-frequency power (kW)	1.35
Carrier gas (Ar) flow rate (L/min)	1.0
Auxiliary gas (Ar) flow rate (L/min)	0.6
Coolant gas (Ar) flow rate (L/min)	16
Nebulizer flow (psi)	20
Pump rate (rpm)	120
Observation height (mm)	15
Sample uptake rate (mL/min)	1.5
Wavelength (nm)	Pb(II): 216.999, Cd(II): 214.438

Brunauer–Emmett–Teller specific surface area (BET) and micropore surface area, were obtained from nitrogen adsorption in the relative pressure range from 0.05 to 0.99 with Quantachrome QuadraWin. Multipoint Brunauer–Emmett–Teller (3H-2000BET, Beishide Instrument-S&T. Co., Ltd., Beijing, China) of CCS was 42.53 m^2/g. The Barrett-Joyner-Hallenda (BJH) method cumulative desorption surface area was 10.95 m^2/g, and the Dubinin-Horvath (DH) method cumulative desorption surface area was 11.24 m^2/g. The total pore volume for pores with a radius (at relative pressure) of 0.987203 was 0.03390 cm^3/g. The BJH method cumulative desorption pore volume was 0.01633 cm^3/g. The DH method cumulative desorption pore volume was 0.01608 cm^3/g. The porosity was 47.44%. The SEM photograph of CCS is shown later in Figure 13.

Adsorption experiments

Standard stock solutions of Pb(II) and Cd(II) were carefully prepared by the dissolution of the spectral pure-grade chemicals $Pb(NO_3)_2$ and $CdCl_2 \cdot H_2O$. They were mixed and diluted into a standard solution containing 100 mg/L Pb(II) and Cd(II) and were further diluted before use as well

All of the adsorption equilibrium experiments were conducted batchwise; the adsorption equilibrium was attained by the shaking of 0.5 g of CCS in 100 mL of aqueous solutions containing metal ions, which were shaken at 250 rpm for a predetermined period. The adsorption experiments were carried out in an incubator at a controlled temperature. After the predetermined adsorption time, the solution was filtered, and the metal-ion concentrations were measured. The initial and equilibrium metal-ion concentrations in the aqueous solutions were determined with an IRIS 1000 Inductively Coupled Plasma Atomic Emission Spectrometer (ICP-AES) (Nicolet Co., Madison Wisconsin in the United States). The relevant operation conditions of the ICP–AES and measurement parameters are summarized in Table I. The initial pH of the solutions was adjusted to the desired pH by the addition of hydrochloric acid or

sodium hydroxide solutions to the medium to maintain a constant pH. A PHS-3C model pH meter (Leici Instrument Factory, Shanghai, China) was used to adjust the pH value. Temperature experiments were carried out between 10 and 40°C at optimum pH values for each metal ion. The amount of adsorbed metal ion was calculated from the change in the metal concentration in the aqueous solution before and after equilibrium and the weight of the dry starch. The amount of metal ion adsorbed by CCS was calculated as follows:

$$Q = \frac{(C_0 - C_t) \times V}{m} \qquad (1)$$

where Q is the amount of metal ion adsorbed onto a unit amount of CCS (mg/g), C_0 and C_t (mg/L) are the concentration of metal ions in the aqueous phase at the initial time and at time t, respectively, V is the total volume of the aqueous solution (L), and m is the dry weight of CCS (g).

All of the experiments were repeated three times, and the average values are presented in this communication. Blank experiments were carried out to ensure that no adsorption was taking place on the walls of the apparatus used.

RESULTS AND DISCUSSION

Effect of pH

CCS, with its polymeric structure, has hydroxyl, carboxyl, and ether functional groups in various proportions. Because of the protonation and deprotonation of those functional groups on the surface of CCS, its adsorption behavior for metal ions is influenced by the pH value. Thus, variation of the metal adsorption with pH is shown in Figure 1. The tests were limited to the pH range 3.0–7.0 because of the precipitation of
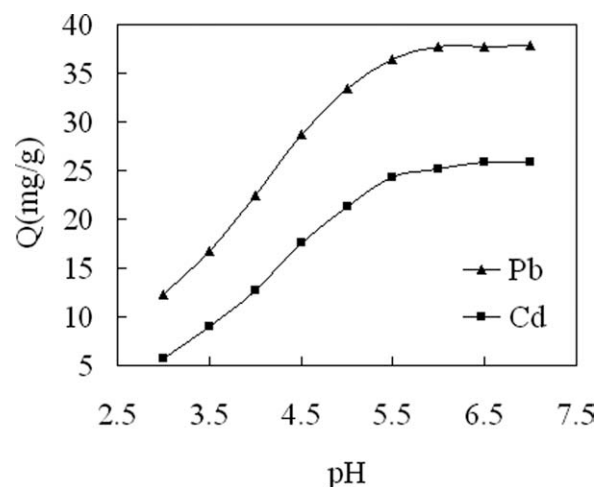
Figure 1 Effect of pH on the adsorption capacity of Pb(II) and Cd(II) ions on CCS at 25°C at an initial concentration of 200 mg/L.
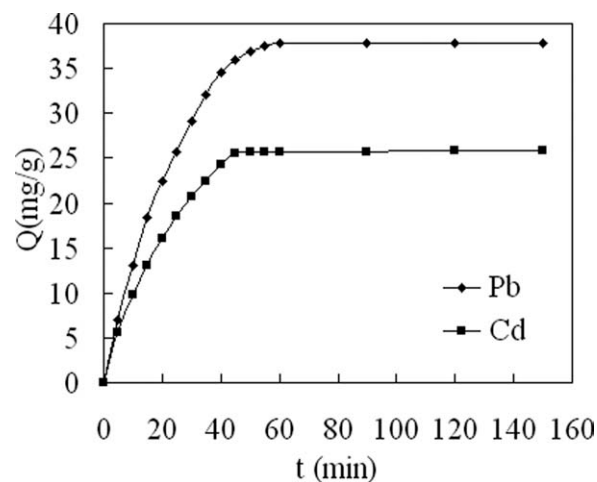
Figure 2 Effect of the contact time on the adsorption capacity of Pb(II) and Cd(II) ions on CCS at 25°C at an initial concentration of 200 mg/L and optimum pH.

Pb(II) and Cd(II) ions; as a matter of fact, hydroxide formed above pH 7.0. For Pb(II) and Cd(II) ions, the adsorption capacity increased with increasing pH and reached a plateau value around pH 6.5 and 7.0, respectively. Ünlü and Ersoz[17] showed that removal of Pb(II) and Cd(II) ions on sporopollenin was completed at pH 6.0 and 7.0, respectively. From Figure 1, it was found that in a strongly acidic solution, CCS had a lower adsorption capacity. This could be explained by the competitive adsorption of H_3O^+ ions and metal ions for the same active adsorption site. Then, cationic repulsion could occur between metal-ion species and protonated carboxymethyl groups on starch chains. As the pH increased, the adsorption surface became less positive, and therefore, the electrostatic attraction between the metal ions and the CCS surface was likely to be increased. Also, this may have been further explained by the functional groups present on CCS.

Effect of the contact time

Figure 2 shows the time course of the adsorption equilibrium of Pb(II) and Cd(II) ions onto CCS. As shown in Figure 2, the adsorption rate was very rapid within 45 min, after which time adsorption continued to occur, but the trend of the increase was very slow. The adsorption became almost constant after 1 h. Therefore, 1 h of contact time was chosen as the optimum equilibration time for the experimental studies, unless otherwise stated, to ensure that equilibrium conditions were achieved. The adsorption results indicate the adsorption of metal ions was fast at the initial stages of the treatment time, and thereafter, it become slower near the equilibrium. It was obvious that a large number of vacant surface sites were available for adsorption during the initial stage, and after a lapse of time, the remaining vacant surface sites
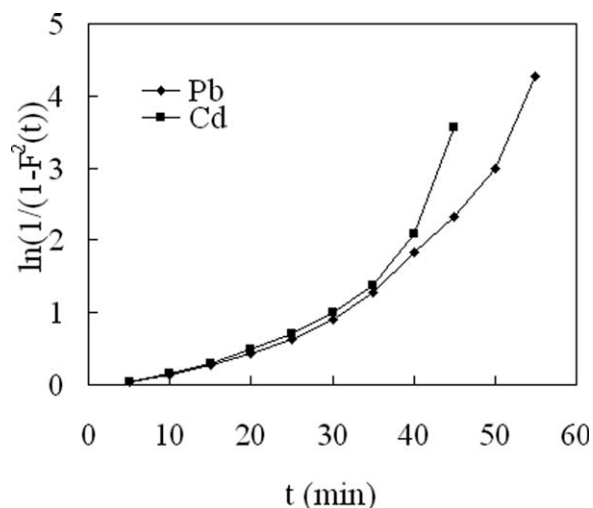
Figure 3 External diffusion plots for the adsorption of Pb(II) and Cd(II) ions on CCS.

were difficult to occupy because of repulsive forces between metal ions adsorbed on the solid and solution phases. It is evident from Figure 2 that the removal efficiency of the adsorbent reached 94.45% for Pb(II) ions and 64.73% for Cd(II) ions at 60 min. With the increase in the amount of adsorbent, the removal efficiency increased.

The kinetic characteristics of a chelating polymer depend not only on the presence of chelating functional groups on it but also on the accessibility of the functional groups without steric hindrance; this is greatly determined by the polymeric matrices. Also, the adsorbents with the best characteristics are those based on hydrophilic macroporous structures. Starch's porous, hydrophilic structure, which shows good permeability functionality and easily available chelating functional groups, were thought to be responsible for these rapid uptake kinetics.

It is known that the adsorption process on adsorbents could be dependent on and controlled with different kinds of mechanisms. To clarify the adsorption process, several adsorption models were applied to evaluate the experimental data. For this purpose, the external diffusion model, intraparticle diffusion model, pseudo-first-order kinetic model, and pseudo-second-order kinetic model were used.

Adsorption kinetics

In general, there are three main steps involved in metal-ion sorption onto a solid sorbent: (1) the transport of metal ions from the bulk solution to the sorbent surface, (2) adsorption on the particle surface, and (3) transport within the sorbent particle. Adsorption studies, in particular, kinetics and isotherms, provide information on the mechanism of sorption: how are metal ions bound within the ab-

sorbent? This knowledge is essential for understanding the sorption process and for selecting the adsorption strategy.

External diffusion model

If the external diffusion of metal ions (within the diffuse layers outside the adsorbent) is the rate-limiting step, it has been shown that eq. (2) can be fitted into the adsorption data with some success:[18]

$$\ln \frac{1}{[1 - F^2(t)]} = k_{ed}t \qquad (2)$$

where $F(t) = Q_t/Q_e$ is the fractional attainment of equilibrium at time t [where Q_t is the amount of metal ions adsorbed at time t (mg/g) and Q_e is the amount of Pb(II) and Cd(II) adsorbed at equilibrium (mg/g)], and k_{ed} is the effective diffusion coefficient of adsorbates in the adsorbent phase (min^{-1}). k_{ed} can be calculated from the slope of the plot of $\ln\{1/[1 - F^2(t)]\}$ versus t (Figure 3). Table II also presents the values of k_{ed}. The values of k_{ed} were found to be 0.0768 and 0.0752/min, respectively, for the adsorption of Pb(II) and Cd(II) ions onto CCS. This showed that the Pb(II) ions had the highest overall pore diffusion rate.

Intraparticle diffusion

For porous surfaces, in the aqueous phase, the pore surfaces are hydrated; this potentially results in layers of water adsorbed to these pore walls. Therefore, the pores may act as micropores. Both pore and surface diffusion may play a role in the liquid-phase adsorption on macroporous adsorbents. Because, for metal-ion adsorption onto starch with a

TABLE II
Kinetic Parameters for the Adsorption of Pb(II) and Cd(II) Ions on CCS

Kinetic equation	Pb(II) ions	Cd(II) ions
External diffusion model		
K_f (min^{-1})	0.0768	0.0752
R^2	0.8840	0.8216
Intraparticle diffusion parameters		
$k_{id,1}$ (mg g^{-1} min$^{0.5}$)	6.7962	4.5208
R^2	0.9997	0.9989
$k_{id,2}$ (mg g^{-1} min$^{0.5}$)	2.6507	0.140
R^2	0.9883	0.8945
Pseudo-first-order model		
k_1 (min^{-1})	0.0741	0.0709
Q_m (mg/g)	56.81	35.54
R^2	0.9626	0.9476
Pseudo-second-order model		
k_2 (g mg^{-1}/min)	2.84×10^{-4}	5.66×10^{-4}
Q_m (mg/g)	74.63	46.73
R^2	0.9953	0.9980
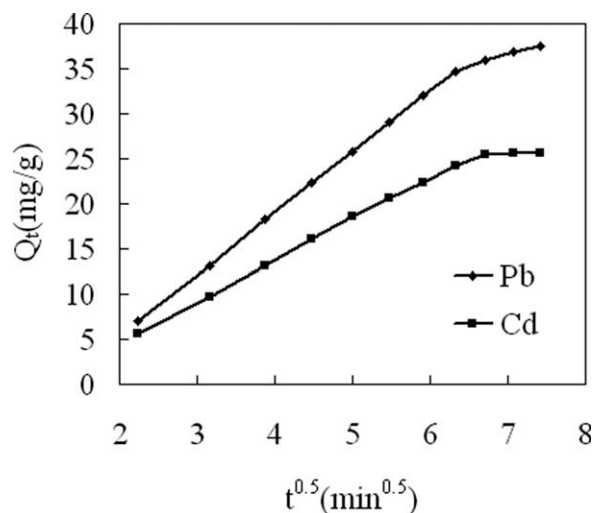
Figure 4 Intraparticle diffusion plots for the adsorption of Pb(II) and Cd(II) ions on CCS.
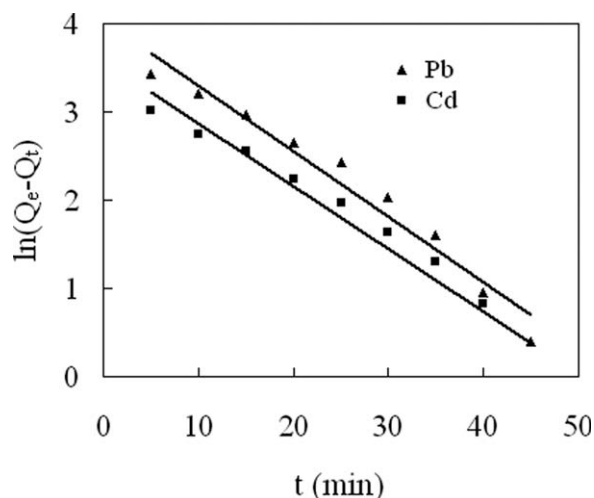
porous structure, kinetic studies have to be done to determine the effects of intraparticle diffusion to the adsorption process.

The intraparticle diffusion model is expressed with the equation given by Bakouri et al.:[19]

$$Q_t = k_{id}t^{0.5} \tag{3}$$

where k_{id} is the intraparticle diffusion rate constant (mg g^{-1}/min$^{/2}$). Plots of Q_t versus $t^{0.5}$ are shown in Figure 4.

As can be seen from Figure 4, for Pb(II) and Cd(II) ions, the data points were related by two straight lines, with the first straight portion depicting macropore diffusion and the second representing mesopore diffusion. The intraparticle diffusion rate constants ($k_{id,1}$ and $k_{id,2}$) were calculated from the slopes of the two linear portions of the curves and are given in

Table II. The first, sharper portion showed that the macropore diffusion onto the particles was significant in the early stages of adsorption. The second, linear portion was the gradual adsorption stage, with intraparticle diffusion dominating. The results show that intraparticle diffusion may have played an important role as a rate-determining step in the adsorption process. However, because of the deviation of the curves from the origin due to the difference in the rate of mass transfer in the initial and final stages of adsorption, intraparticle diffusion could not be accepted as the only rate-determining step for the adsorption of those target heavy metal ions onto CCS. From Table II, k_{id} is much higher for Pb(II) than for Cd(II) because of its relatively small hydrated radius.

Pseudo-first-order model

The pseudo-first-order model considers that the rate of occupation of adsorption sites is proportional to the number of unoccupied sites. With first-order kinetics, the fractional uptake of the adsorbate by the adsorbent can be expressed as follows:[20]

$$\ln(Q_e - Q_t) = \ln Q_e - kt \tag{4}$$

where k is the adsorption constant of first-order sorption (min^{-1}).

When plotted as $\ln(Q_e - Q_t)$ versus t (Figure 5) for the adsorption of metal ions at 25°C, the values of k and the predicted maximum adsorption capacity (Q_m) values obtained from the pseudo-first-order kinetic models are listed in Table II. From Table II, for Cd, Q_m was 35.54, and for Pb, Q_m was 56.81 mg/g; these values were too low compared with experimental Q_m values in Figure 6. From Figure 6, for Cd, Q_m was about 43, and for Pb, Q_m was about

Figure 5 Pseudo-first-order plots for the adsorption of Pb(II) and Cd(II) ions on CCS.
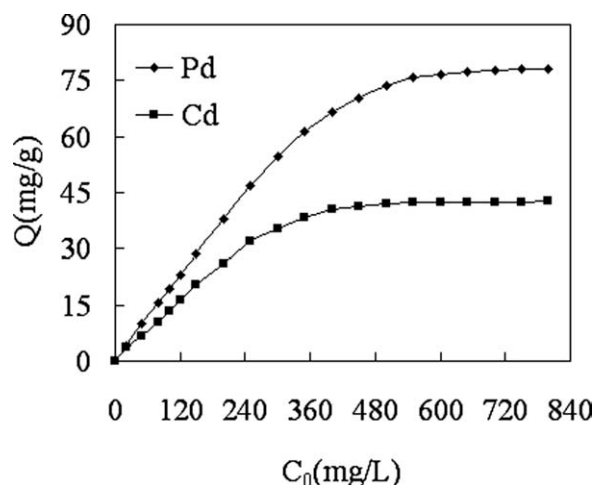
Figure 6 Effect of the initial concentration on the adsorption of Pb(II) and Cd(II) ions on CCS at 25°C and optimum pH
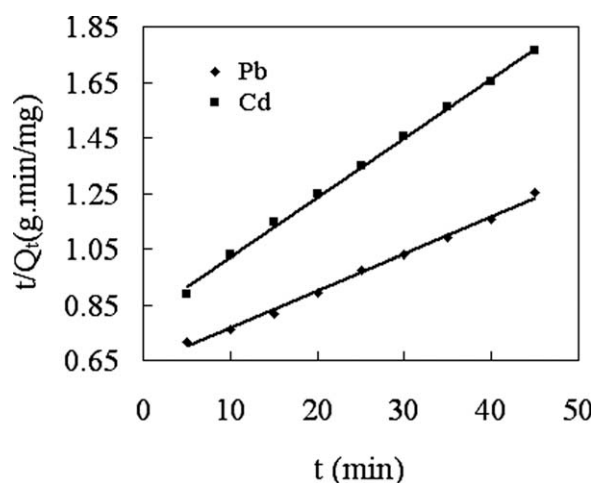
Figure 7 Pseudo-second-order plots for the adsorption of Pb(II) and Cd(II) ions on CCS.

78 mg/g. This finding suggests that the process of the adsorption of Pb(II) and Cd(II) on CCS did not follow the pseudo-first-order adsorption rate expression. Therefore, any reaction occurring was not likely to be a first-order reaction.

Pseudo-second-order model

A pseudo-second-order model may also describe the kinetics of adsorption. The rate of pseudo-second-order reaction was dependent on the amount of Pb(II) and Cd(II) adsorbed on the surface of adsorbent and the amount adsorbed at equilibrium. The pseudo-second-order model[21] can be expressed as follows:

$$\frac{t}{Q_t} = \frac{1}{k_2 Q_e^2} + \frac{1}{Q_e} t \qquad (5)$$

where k_2 is the rate constant of the adsorption (g mg^{-1} min^{-1}), Q_e is the amount of Pb(II) and Cd(II) adsorbed at equilibrium (mg/g), Q_t is the amount of adsorbed Pb(II) and Cd(II) on starch at any time t (mg/g), and $k_2 Q_e^2$ is the initial adsorption rate (h).

　Figure 7 shows the plot of t/Q_t versus t for the adsorption of metal ions on CCS. The values of k and Q_m could be obtained from the intercept and the slope of the line and are listed in Table II. The adsorption data did fit as the line passed through entire points, with a correlation coefficient (R^2) relatively close to 1.00. From Table II, for Cd, Q_m was about 46.73, and for Pb, Q_m was about 74.63 mg/g; the predicted Q_m values obtained from the pseudo-second-order kinetic models were closer than those of the pseudo-first-order kinetic model to the experimental Q_m values. Both facts suggest that the adsorption of metal ions followed the pseudo-second-order model, which relies on the assumption that chemical adsorption involving valency forces between the

hydrophilic functional groups and metal cations may be the rate-limiting step. It is possible to say that the metal ions adsorbed on anionic carboxyl groups absorbed in CCS via chemical bonds.

**Effect of the initial metal-ion concentration**

Adsorption equilibrium data are mainly about the adsorption capacities of the adsorbents at different metal-ion concentrations. The effect of the initial concentration on the adsorption capacity is shown in Figure 6. As can be seen from Figure 6, the equilibrium adsorption capacities of CCS for Pb(II) and Cd(II) ions increased with increasing initial concentration; this meant that the adsorption process was highly concentration dependent. When the initial concentration was increased from 200 up to 600 mg/L, the adsorption capacities of CCS for Pb(II) and Cd(II) ions increased from 37.78 to 76.53 mg/g and from 25.89 to 42.27 mg/g, respectively. The increase in the adsorption capacity of CCS with relation to metal-ion concentration was probably due to a high driving force for mass transfer. However, there was little increase in the adsorption capacity for initial concentration changes beyond 600 mg/L. The adsorption performance of metal ions on CCS mainly depended on the active carboxymethyl groups. The adsorption capacities, therefore, tended toward saturated values with a decrease in the content of available carboxymethyl groups. From Figure 6, the experimental values of the maximal adsorption capacities of CCS (Q_m) were about 78 and 43 mg/g for the Pb(II) and Cd(II) ions, respectively. Wan Ngah and Fatinathan[22] reported that the value of maximum adsorption capacity of chitosan–tripolyphosphate beads for Pb(II) ions was 57.33 mg/g at 300 K. Xie et al.[14] reported that the value of maximum adsorption capacity of amino-modified starch for Cd(II) ions was 54.06 mg/g.

Adsorption isotherms

Equilibrium adsorption isotherms relate the adsorbate concentration in the bulk to the adsorbed amount on the interface. The analysis of the isotherm data is important for developing an equation that accurately represents the results and that could be used for design purposes. Experimental data obtained from the effect of the initial concentration on the adsorption capacity were evaluated with the three popular adsorption models, the Langmuir, Freundlich, and D–R isotherm models. The linearized forms of the equations representing the models were used.

Langmuir isotherm

The Langmuir isotherm has been widely used to describe single-solute systems. It is based on the
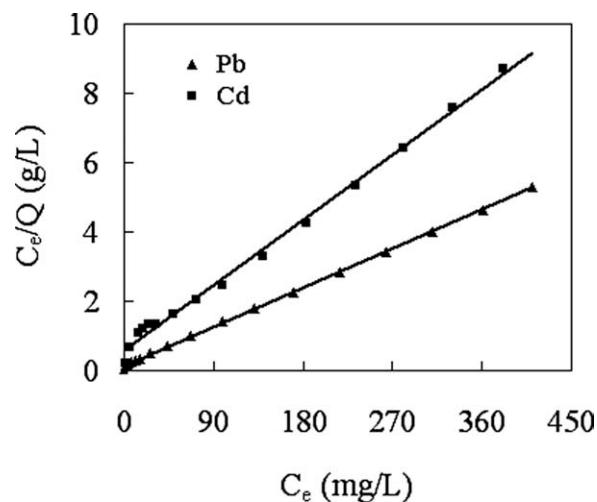
Figure 8 Langmuir isotherm for the adsorption of Pb(II) and Cd(II) ions on CCS at 25°C and optimum pH.

assumption that intermolecular forces decrease rapidly with distance, and consequently, it predicts monolayer coverage of the adsorbate on the outer surface of the adsorbent. The isotherm equation further assumes that adsorption takes place at specific homogeneous sites within the adsorbent and that there is no significant interaction among the adsorbed species. Theoretically, the adsorbent has a finite capacity for the adsorbate. Once a metal ion occupies a site, no further adsorption can take place at that site. The Langmuir model is written as follows:[23]

$$\frac{C_e}{Q} = \frac{1}{Q_m b} + \frac{C_e}{Q_m} \tag{6}$$

where C_e is the equilibrium concentration of metal ions (mg/L) in the solution, Q is the adsorbed amount of metal ions (mg/g), Q_m represents the maximum amount of adsorbed metal ions (mg/g), and b is the Langmuir constant, which is related to the energy of adsorption (L/mg).

Figure 8 shows the experimental data fitted to the linear form of the Langmuir isotherm for Pb(II) and Cd(II) ion adsorption by CCS. The values of Q_m and b were calculated from the slope and the intercept of the linear plot of C_e/Q versus C_e and are also listed in Table III.

As shown in Table III, the R^2 values obtained from the Langmuir model were 0.9993 and 0.9954 for Pb(II) and Cd(II) ions, respectively, and the Q_m values were 80.0 and 47.85 mg/g for Pb(II) and Cd(II) ions, respectively; these values suggested that the adsorption of metal ions onto CCS closely followed the Langmuir model. The b values obtained from the Langmuir model [9.84 and 2.72 L/mg for Pb(II) and Cd(II) ions, respectively] suggested that the metal binding affinity was in the order Pb(II) > Cd(II).

The effect of isotherm shape can be used to predict whether an adsorption system is favorable or unfavorable. According to Gupta et al.,[24] the essential features of the Langmuir isotherm can be expressed in terms of a dimensionless constant separation factor or equilibrium parameter (K_R), which is defined by the following relationship:

$$K_R = \frac{1}{1 + bC_0} \tag{7}$$

The value of K_R indicates the type of the isotherm to be unfavorable ($K_R > 1$), linear ($K_R = 1$), favorable ($0 < K_R < 1$), or irreversible ($K_R = 0$).

The values of K_R at 25°C for the adsorption of Pb(II) ions by CCS decreased from 0.00203 to 0.000203, whereas the initial concentration of Cd(II) increased from 50 to 500 mg/L. The values of K_R at 25°C for the adsorption of Cd(II) ions decreased from 0.00730 to 0.000735. The K_R values were found to be less than 1 and greater than 0 for all experiments carried out at different initial concentrations. These results show that Pb(II) and Cd(II) ion adsorption on CCS was more favorable at the higher initial concentration.
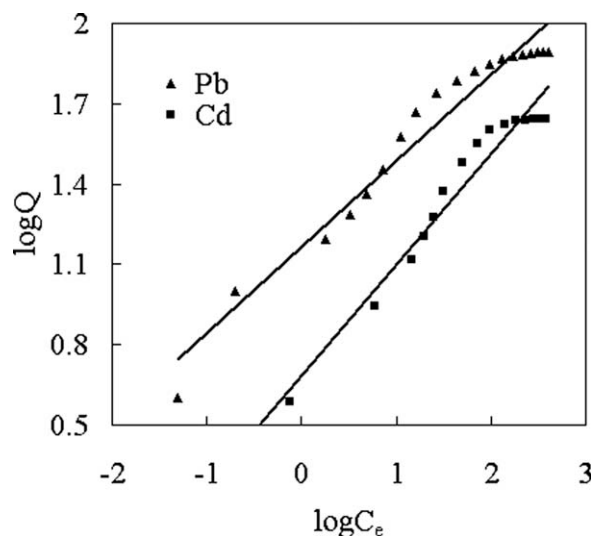
Freundlich isotherm

The empirical Freundlich isotherm is based on adsorption on a heterogeneous surface and is expressed by the following equation:

$$\log Q = \log K_f + \frac{1}{n} \log C_e \tag{8}$$

where K_f is the proportionality constant, which is indicative of bond strength, and n is a dimensionless exponent related to the bond energies between the metal ion and the adsorbents.

TABLE III
Isotherm Constants for the Adsorption of Pb(II) and Cd(II) Ions on CCS

Isotherm equation	Pb(II) ions	Cd(II) ions
Langmuir isotherm		
Q_m (mg/g)	80.0	47.85
b (L/mg)	9.84	2.72
R^2	0.9993	0.9954
Freundlich isotherm		
$K_f \times 10^{-3}$ (L/mg)$^{1/n}$	14.52	4.82
n	3.11	2.41
R^2	0.9546	0.9527
D–R		
Q_m (mg/g)	79.65	46.09
k (mol/kJ)^2	0.0059	0.0077
E (kJ/mol)	9.21	8.06
R^2	0.9881	0.9625

Figure 9 Freundlich isotherm for the adsorption of Pb(II) and Cd(II) ions on CCS at 25°C and optimum pH.

The values of K_f and n were calculated from the slope and the intercept of the linear plot between $-\log Q$ and $-\log C_e$ (Figure 9) and are presented in Table III.

As shown in Table III, the R^2 values obtained from the Freundlich model were 0.9546 and 0.9527 for Pb(II) and Cd(II) ions, respectively. The result also suggests that the adsorption system of CCS could have had more than one functional group, which was responsible for the metal binding. Moreover, the magnitude of K_f [14.52×10^{-3} and 4.82×10^{-3} (L/mg)$^{1/n}$ for Pb(II) and Cd(II) ions, respectively] obtained from the Freundlich model also supported the fact that the metal binding affinity was in the order Pb(II) > Cd(II). From Table III, it is evident that the n values (>3.1) for Pb(II) were higher than those of Cd(II) ($n > 2.4$); this indicated stronger bond energy between the Pb(II) ions and CCS as compared to that between the Cd(II) ions and CCS.

D–R isotherm

The Langmuir and Freundlich isotherms do not give any ideas about the adsorption mechanism. The D–R isotherm describes adsorption on a single type of uniform pore. In this respect, the D–R isotherm is an analog of Langmuir type, but it is more general because it does not assume a homogeneous surface or a constant sorption potential. To understand the adsorption type, the D–R isotherms were obtained. The D–R isotherm is given by the following equation:[22]

$$Q = Q_m \exp(-k\varepsilon^2) \tag{9}$$

The linearized form of the equation is given as follows:

$$\ln Q = \ln Q_m - k\varepsilon^2 \tag{10}$$

where ε is the Polanyi potential, calculated as $\{RT \ln[1 + (1/C_e)]\}$, Q is the amount of solute adsorbed per unit weight of adsorbent (mg/g), k is a constant related to the adsorption energy (mol^2/kJ^2), and Q_m is the adsorption capacity (mg/g).

The values of Q_m and k were calculated from the intercept and slope of the ln Q versus ε^2 plots (Figure 10) and are presented in Table III. From Table III, the Q_m values obtained from the D–R isotherm were in agreement with the experimental Q_m values. The mean free energy of adsorption (E) was calculated from the k values with the following equation:

$$E = (-2k)^{-0.5} \tag{11}$$

The magnitude of E is useful for estimating the type of adsorption process. If this value is between 8 and 16 kJ/mol, the adsorption process can be explained by ion exchange. In this study, the E values were calculated to be between the values of ion exchange. Therefore, it is possible to say that the adsorption mechanism of the Pb(II) and Cd(II) ions on CCS could be explained by an ion-exchange process.

Thermodynamics of the adsorption

To explain the effect of the temperature on the adsorption, the adsorption capacity of CCS for metal ions at various temperature (15–35°C) were determined. A plot of the relation of the two variables showed a decreasing trend (Figure 11). An increase in the temperature decreased the adsorption performance. This was consistent with the fact that adsorption is an exothermic process, and therefore, the rise in temperature suppressed the metal uptake. To verify the conclusion, $\log(Q/C_e)$ was plotted
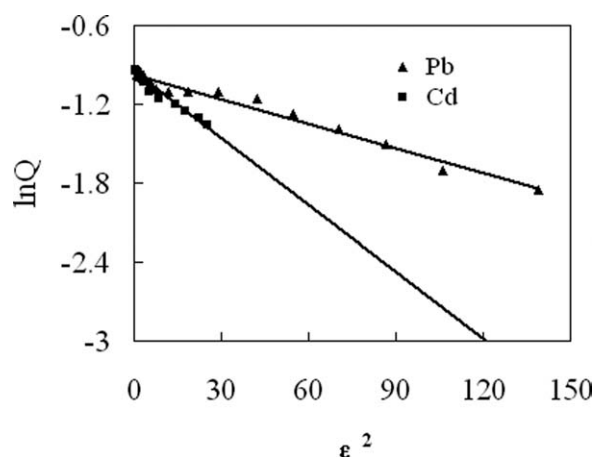
Figure 10 D–R plots for the adsorption of Pb(II) and Cd(II) ions on CCS at 25°C and optimum pH.
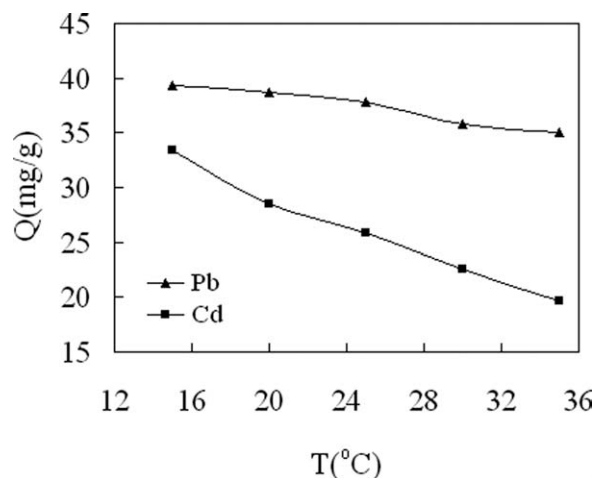
Figure 11 Effect of the temperature on the adsorption capacity of Pb(II) and Cd(II) ions at an initial concentration of 200 mg/L and optimum pH.

versus $1/T$ (Figure 12) to give the apparent enthalpy change (ΔH^θ) and ΔS^θ according to the following equation:
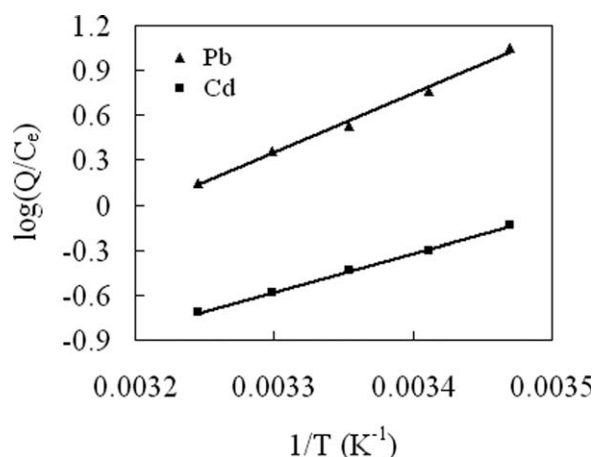
$$\log \frac{Q}{C_e} = -\frac{\Delta H^\theta}{2.303RT} + \frac{\Delta S^\theta}{R} \tag{12}$$

T is temperature (K), ΔG^θ was calculated with the following relationship and is listed in Table IV:

$$\Delta G^\theta = \Delta H^\theta - T\Delta S^\theta \tag{13}$$

It could be observed that the adsorption capacities decreased as the temperature increased. As reflected from the negative value of ΔH^θ, the adsorption process was exothermic; this was responsible for the reduction in adsorption as the temperature increased.

Thermodynamic considerations tell us that at a constant temperature and pressure, ΔG^θ during the spontaneous adsorption process always has a negative sign. However, from a more random state (in solution) to a more orderly state (on the surface of the adsorbent) for metal ions, ΔS^θ also has a negative sign. As known from thermodynamics, negative values of ΔG^θ and ΔS^θ require a negative adsorption enthalpy (ΔH^θ), which eventually implies that the adsorption phenomenon is exothermic. In Table IV, the negative ΔG^θ values show the spontaneity of the adsorption process. ΔG^θ was more negative with decreasing temperature, which suggested that a lower temperature made the adsorption easier.

The ΔH^θ value can be used as a measure of the interaction force between an adsorbate and adsorbent. In the adsorption of metal ions, the net ΔH^θ and ΔS^θ values of the adsorption are the result of different processes. The dehydration form of the metal ion with water generally involves a positive ΔH^θ ($\Delta H^\theta > 0$) as a result of the breakage of ion–water bonds and a positive ΔS^θ ($\Delta S^\theta > 0$) because of an increase of disorder in the system by the release of bonded water. However, complexes formed with carboxyl groups will result in a negative ΔH^θ ($<$) as a consequence of the replacement of relatively weak hydrogen bonds with stronger metal bonds and in a negative ΔS^θ ($\Delta S^\theta < 0$) because of the increase of order caused by the new bonds. The ΔH^θ and ΔS^θ values found in this experiment showed that the newly formed bond between metal ions and CCS was stronger than the bond between hydrogen ions and CCS. Also, the metal-ion binding mechanism could be explained by the interaction between metal ions and carboxyl groups derived from chemical interaction, and the adsorption reaction taking place with the replacement of protons by the metal ions. These findings agreed with the experimental results.

Adsorption on a solid is classified into physical adsorption and chemical adsorption. Physical adsorption is nonspecific, and the ΔH^θ values for chemical adsorption are usually substantially greater

Figure 12 Plot of $\log(Q/C_e)$ versus $1/T$ for the adsorption of Pb(II) and Cd(II) ions on CCS.

TABLE IV
Thermodynamic Parameters for the Adsorption of Pb(II) and Cd(II) Ions on CCS

Metal ions	Temperature (°C)	ΔG^θ (kJ/mol)	ΔH^θ (kJ/mol)	ΔS^θ (J mol^{-1} K^{-1})	R^2
Pb	15	−44.99	−75.20	−104.84	0.9948
	20	−44.47	−75.20	−104.84	
	25	−43.94	−75.20	−104.84	
	30	−43.42	−75.20	−104.84	
	35	−42.89	−75.20	−104.84	
Cd	15	−27.40	−49.03	−75.07	0.9983
	20	−27.02	−49.03	−75.07	
	25	−26.65	−49.03	−75.07	
	30	−26.27	−49.03	−75.07	
	35	−25.90	−49.03	−75.07	
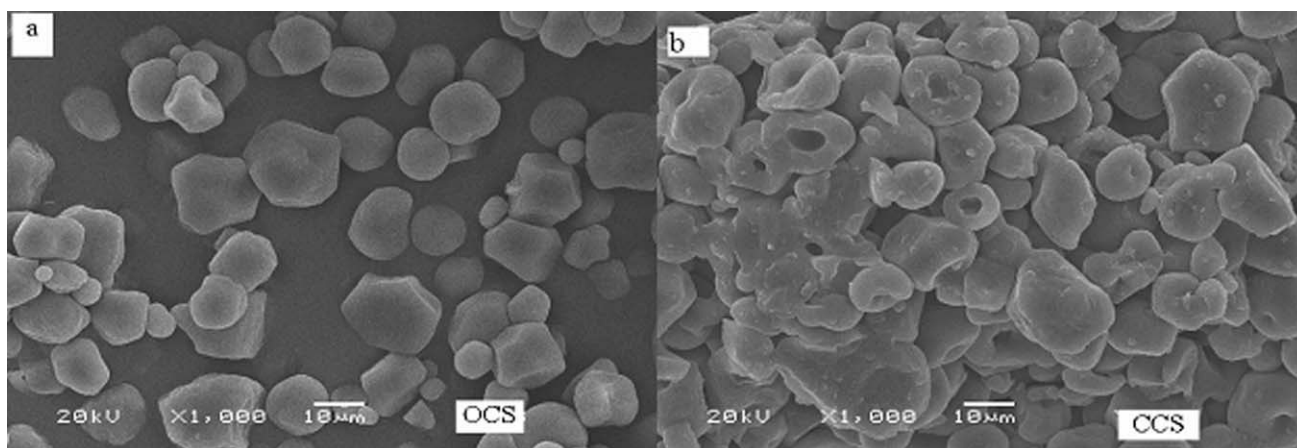
Figure 13 SEM photographs of (a) original corn starch and (b) CCS.

in magnitude than those for physical adsorption. As seen from Table IV, the ΔH^{θ} values for Pb(II) and Cd(II) ions were −75.20 and −49.03 kJ/mol, respectively; these values were slightly higher than those of the lower limit corresponding to chemical adsorption. This indicated that the chemical adsorption process was involved in the Pb(II) and Cd(II) ion sorption on CCS.

SEM photographs of the original corn starch and CCS

SEM photographs clearly show the structures of the original corn starch and CCS in Figure 13. It can be seen that the surfaces of the original corn starch particles [Figure 13(a)] were smooth; however, the cleavage of glucosidal rings for particles carboxymethylated in alkaline conditions produced and led to an uneven surface and created pores on the particles [Figure 13(b)]. Furthermore, the particles were conglomerated closely, and the granules became much bigger than the original starch.

CONCLUSIONS

It has been determined that the adsorption capacities of CCS for metal ions depended on the pH, contact time, initial metal-ion concentration, and temperature. The kinetic studies indicated that intraparticle diffusion was found to take part in the adsorption processes, but it could not be accepted as the only rate-determining step. Regardless of the metal type, the pseudo-second-order chemical reaction kinetics were able to provide a realistic description of the adsorption kinetics of metal ions on CCS. Adsorption isotherm models were developed wherein the better fit was obtained in the Langmuir model and the D–R isotherm. The maximum loading capacities of CCS were about 80.0 and 47.0 mg/g for the Pb(II)

and Cd(II) ions, respectively. The E values were found to be between 8 and 16 kJ/mol for the metal ions studied, and therefore, the adsorption mechanism for the adsorbent was explained as an ion-exchange process.

On the basis of the thermodynamic studies, it was found that the adsorption process was spontaneous and exothermic in nature. The ΔH^{θ} values for Pb(II) and Cd(II) ion adsorption under investigation were −75.20 and −49.03 kJ/mol, respectively, in which the adsorption of Pb (II) and Cd(II) by CCS could be considered a chemical sorption process simultaneously enhanced by the ion-exchange effect, and the Pb(II) and Cd(II) ions adsorption capacities on CCS decreased in the order Pb(II) > Cd(II). The adsorption experiments showed that CCS could be used as an effective adsorbent for the removal of Pb(II) and Cd(II) ions. The studies of the kinetics, isotherms, and thermodynamics indicated that the adsorption of CCS for Pb(II) ions was more effective than that for Cd(II) ions.

References

1. Abbas, M.; Zaini, A.; Amano, Y.; Machida, M. J Hazard Mater 2010, 180, 552.
2. Hu, Z.; Lei, L.; Li, Y.; Ni, Y. Sep Purif Technol 2003, 31, 13.
3. Ijagbemi, C. O.; Baek, M. H.; Kim, D. S. J Hazard Mater 2009, 166, 538.
4. Šćiban, M.; Klašnja, M.; Škrbić, B. Desalination 2008, 229, 170.
5. Lopez, F. A.; Martin, M. I.; Pérez, C.; Lopez-Delgado, A.; Alguacil, F. J. Water Res 2003, 37, 3883.
6. Krishnapriya, K. R.; Kandaswamy, M. Carbohydr Res 2010, 345, 2013.
7. Homagai, P. L.; Ghimire, K. N.; Inoue, K. Bioresour Technol 2010, 101, 2067.
8. Atia, A.; Donia, A. M.; Abou-El-Enein, S. A. Sep Purif Technol 2003, 33, 295.
9. Azanova, V. V.; Hradil, J. React Funct Polym 1999, 41, 163.
10. Zhang, L. M.; Chen, D. Q. Colloids Surf A 2002, 205, 231.
11. Dong, A.; Xie, J.; Wang, W.; Yu, L.; Liu, Q.; Yin, Y. J Hazard Mater 2010, 181, 448.

12. Guo, L.; Sun, C.; Li, G.; Liu, C.; Ji, C. J Hazard Mater 2009, 161, 510.
13. Ding, W.; Zhao, P.; Li, R. Carbohydr Polym 2011, 83, 802.
14. Xie, G.; Shang, X.; Liu, R.; Hu, J.; Liao, S. Carbohydr Polym 2011, 84, 430.
15. Chen, Y.; Wang, G. Colloids Surf A 2006, 289, 75.
16. Zhang, Y. S. Bianxing Dianfen Shengchan Yu Yingyong Shouce; Zhongguo Qinggongye: Beijing, 1999.
17. Ünlü, N.; Ersoz, M. J Hazard Mater B 2006, 136, 272.
18. Yahya, S.; Al-Degs, M. I.; El-Barghouthi, A. A.; Issa, A. A.; Khraisheh, G. M. Water Res 2006, 40, 2645.
19. Bakouri, H. E.; Usero, J.; Morillo, J.; Rojas, R.; Ouassini, A. Bioresour Technol 2009, 100, 2676.
20. Ferrah, N.; Abderrahim, O.; Didi, M. A. Desalination 2011, 269, 17.
21. Kundu, S.; Gupta, A. K. Colloids Surf A 2006, 273, 121.
22. Wan Ngah, W. S.; Fatinathan, S. J Environ Manage 2010, 91, 958.
23. Chen, Y.; Wang, G. J Appl Polym Sci 2006, 102, 1539.
24. Gupta, V. K.; Mittal, A.; Krishnan, L.; Mittal, J. J Colloid Interface Sci 2006, 293, 16.